EFFECT OF SUBSTRATE TEXTURE AND DEPOSITION CURRENT DENSITY ON PROPERTIES OF Ni NANOCRYSTALLINE ELECTRODEPOSITS

M. R. Zamanzad-Ghavidel, K. Raeissi* and A. Saatchi

* *k_raeissi@cc.iut.ac.ir*

Received: November 2011 **Accepted: April 2012**

Department of Materials Engineering, Isfahan University of Technology, Isfahan 84156-83111, Iran.

Abstract: *Nickel was electrodeposited onto copper substrates with high {111} and {400} peak intensities. The grain size of coatings deposited onto the copper substrate with a higher {111} peak intensity was finer. Spheroidized pyramid morphology was obtained at low current densities on both copper substrates. By increasing the deposition current density, grain size of the coating was increased for both substrates and eventually a mixed morphology of pyramids and blocks was appeared without further increase in grain size. This decreased the anodic exchange current density probably due to the decrease of surface roughness and led to a lower corrosion rate.*

Keywords: *Ni Nanocrystalline; Electrodeposition; Texture; Morphology; Corrosion*

1. INTRODUCTION

Electrochemical corrosion performance of nanocrystalline metals and alloys has received a considerable attention in the past decade [1–6]. Generally, in comparison with a conventional coarse-grained pure metal, the general corrosion resistance of the nano-grained counterpart of the same purity was decreased [1-3].

Nickel is widely used as a base metal in the process industry because of its excellent resistance to general corrosion. Corrosion resistance can be affected by microstructure, such as grain size, surface morphology and texture, which is closely related to the electrodeposition parameters, such as current density, pH and electrolyte temperature [5]. Ebrahimi et al. found that the crystallographic texture of the copper substrate significantly affects the properties of nanocrystalline nickel deposits. Annealed copper substrates with {100} planar texture result in deposits with higher strengths and finer crystallite sizes. The deposit fabricated on a cold-rolled copper substrate with {110} texture showed a larger crystallite size and a consistently lower strength [7].

Comparisons of electrochemical corrosion of nanocrystalline Ni with conventional coarse-grained Ni were studied by several investigators [2, 4 - 6, 8]. Rofagha et al. [2] stated that the corrosion rate and passive current density were enhanced in nanocrystalline nickel [2] but Wang et al. [4] found that by decreasing grain size, corrosion rate and passive current density was decreased. Mishra et al. [6] showed that the passive current density was increased by grain refinement but corrosion rate was decreased.

Works on the effect of different microstructure, like grain size, surface morphology and texture on corrosion resistance and pitting susceptibility of nanocrystalline Ni are still lacking and there are a lot of contrarieties. The aim of the present work is to prepare nano and microcrystalline Ni electrodeposits using Watt's bath at different current densities on two copper substrates with different textures and to investigate their corrosion behaviour in 3.5% NaCl solution.

2. EXPERIMENTAL

Electrodeposited Ni was prepared from a Watt's bath containing 240 g l^{-1} $NiSO_4$. $6H_2O$, 30 g l^{-1} $NiCl_2$. $6H_2O$ and 30 g l^{-1} H_3BO_3. Analytical grade (Merck) chemicals and double distilled water were used to prepare the solution. The solution was maintained at pH value of 3.8±0.1 and temperature of 45±1°C. The electrodeposits with the thickness of about 13 μm were obtained at current densities of 2, 10, 20, 30, 50 and 100 mA cm^{-2} by using a BHP 2050 digital coulometer. Microcrystalline electrodeposits were produced by annealing the coating deposited on the copper substrate with a high {111} peak intensity at current density of 100 mA cm^{-2} in a vacuum oven at 850 °C for 1.5 h. The substrates were copper plates with 0.85 cm^2 surface

area in as-rolled condition and copper discs with the same area annealed at 425 °C for 0.5 h. Both copper substrates show almost the same grain size around 38 μm. After grinding up to 600 grit SiC emery paper, the substrates were electropolished potentiostatically at an anodic voltage of 1.3 V for approximately 15 min using a solution containing 82.4% phosphoric acid and 17.5% deionized water at room temperature. After electropolishing, the surface was immediately rinsed and the working electrode was transferred to the deposition cell.

A Philips XL30 scanning electron microscope (SEM) was used to study the coating morphology. Grain size, texture and microstrain were assessed by X-ray diffraction (XRD) technique using a Philips X'pert diffractometer. Texture coefficients (TC) were calculated by using equation (1) for each deposit.

$$TC = \frac{(\frac{I_{hkl}}{I^0_{hkl}})}{\frac{1}{n}\sum_1^n \frac{(I_{hkl})_i}{(I^0_{hkl})_i}} \quad (1)$$

where n is the number of planes which is 4 for Ni, is intensity of {hkl} plane and is intensity of {hkl} at random state. The grain size of the coatings was estimated by applying the Scherrer equation using (200) diffraction peak. The microstrain (ε) in the deposits was calculated through linear fitting of X-ray data. The slope of the plot of B*×cosθ vs. sinθ provides ε according to the following relation [6]:

$$B^* \times \cos\theta = 2\varepsilon \sin\theta + 0.9\lambda / D \quad (2)$$

where B * is the corrected Full-Width at Half Maximum (FWHM), θ is the diffraction angle, D is the grain size and λ (=0.15405 nm) is the wavelength of the radiation used.

In order to observe and evaluate the coating roughness, atomic force microscope (AFM) was used. The images were obtained using a DME DS95-50 scanning probe microscope (Dual Scope C-26) in non-contact mode. Corrosion measurements were performed in a three-electrode cell with the volume of 500 mL of electrolyte. A platinum wire and a saturated calomel electrode (SCE) were used as the auxiliary and reference electrodes, respectively. The electrodes were connected to an EG&G Potentiostat/Galvanostat (model 263A). Corrosion behaviour was examined in stagnant neutral 3.5% NaCl solution at 25 °C. Tafel polarization readings were performed with the scan rate of 1 mV sce^{-1}.

3. RESULTS AND DISCUSSION

3. 1. Substrates

Fig.1 shows X-ray peak intensity pattern of the two copper substrates used in this study, a cold-rolled plate substrate with a strong {400} peak

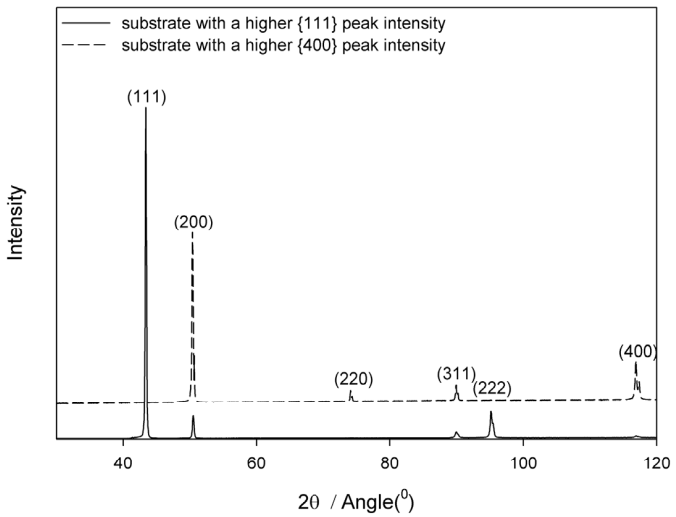

Fig. 1. XRD peak profiles of the copper substrates with two different grain orientations.

intensity and disk shape annealed substrate with a strong {111} peak intensity. It is obvious that these two copper substrates show different texture components.

3. 2. Suitable Current Density for Deposition

Electrodeposition current densities were selected from cathodic polarization readings performed in the electrodepositing bath for each substrate (Fig. 2). Three polarization regions including activation, mixed (activation + diffusion) and diffusion are shown in Fig. 2 for both copper substrates. Current densities of 2 and 10 mA cm^{-2} in the activation polarization region, 20, 30 and 50 mA cm^{-2} in the mixed region and 100 mA cm^{-2} in the diffusion polarization region were selected for coating deposition. As shown in Fig. 2, deposition onto the copper substrate with a higher {400} peak intensity needs to a higher overpotential comparing to the copper substrate with a higher {111} peak intensity.

In FCC metals like Ni, the surface energy of planes increases with their crystallographic index [8]. Higher index of planes (i.e. higher value of $(h^2+k^2+l^2)$) creates lower plane compactness which results in a higher surface energy. In this way, the surface energy of {400} planes is expected to be higher than {111} plane [8]. It is known that the nucleation rate is lower on substrates with higher surface energy [7]. Thus, nucleation of Ni onto the copper substrate with a higher {400} peak intensity is more difficult and accordingly, needs a higher overpotential with respect to the same condition on substrate with a higher {111} peak intensity. This indicates that the frequency of nucleation is lower for the copper substrate with a higher {400} peak intensity. As seen from Fig. 2, this difference on deposition overpotential is reduced by increasing the current density of deposition.

3. 3. Coating Characterization

Figs. 3 and 4 shows the surface morphology of electrodeposits obtained at 2, 10, 20, 30, 50 and 100 mA cm^{-2} on two copper substrates. At 2 mA cm^{-2}, spherical morphology was detected on both copper substrates as seen in Figs. 3a and 4a. Further increase in current density encouraged the formation of a mixed morphology which consists of pyramidal and blocky like regions. The blocky morphology is shown by white arrows in Figs. 3e and 3f and Figs. 4d, 4e and 4f. It is believed that the pyramidal morphology is formed by the transformation of spherical morphology at conditions where H_2 evolutes or solution is highly stirring [9]. It is well known that H_2 evolution is less pronounced at low current densities during the electrodeposition [9].

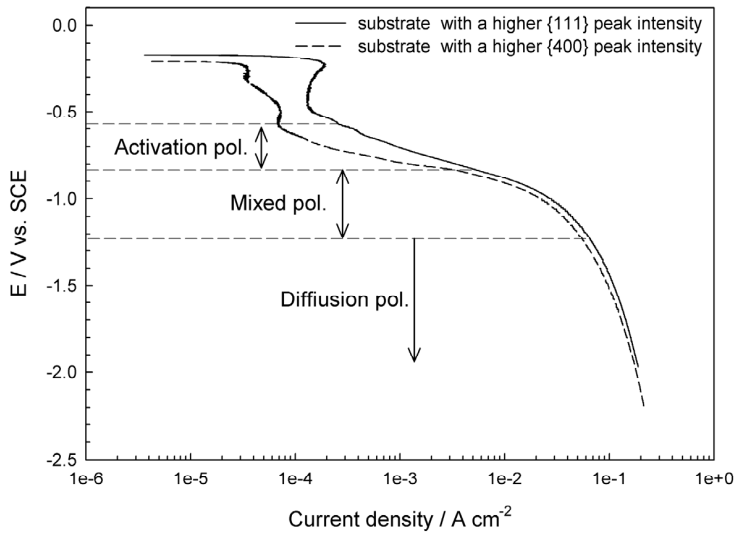

Fig. 2. Cathodic scan plots for two copper substrates (scan rate = 40 mV s^{-1}).

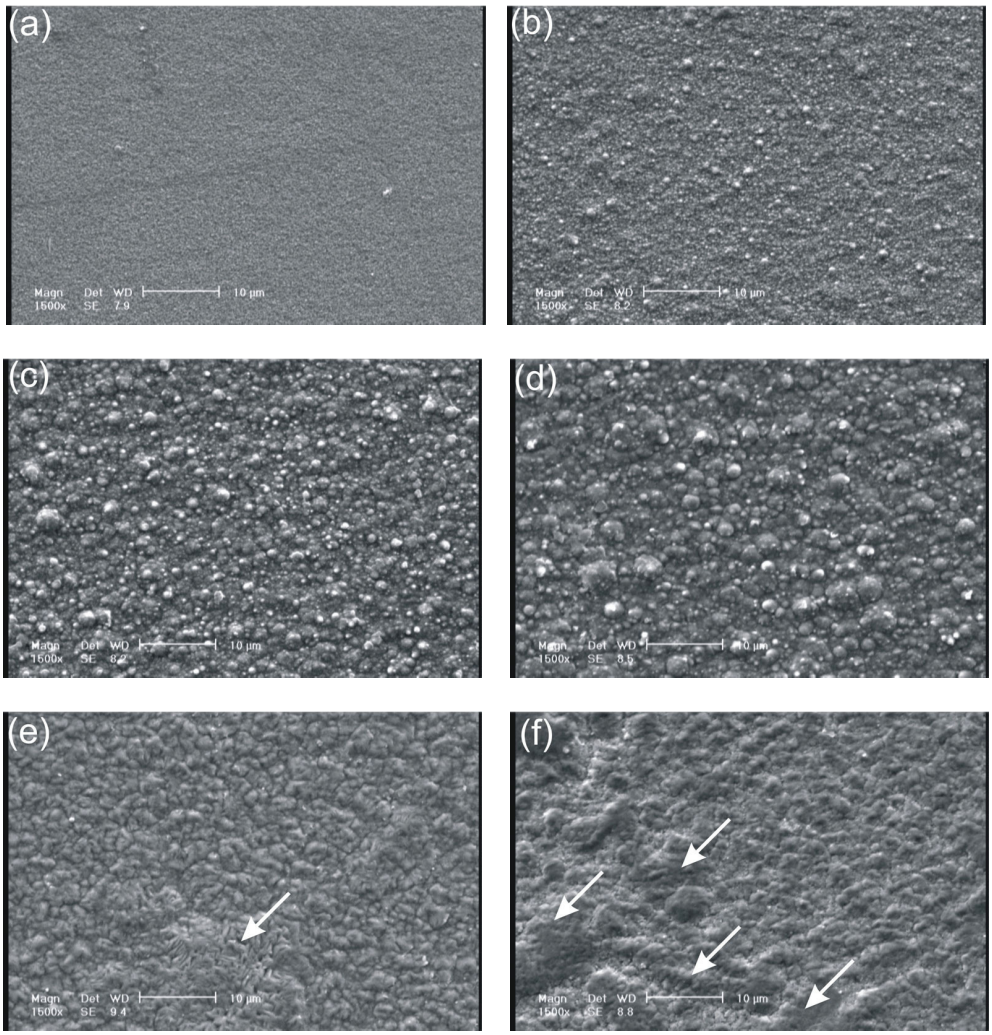

Fig. 3. Surface morphologies of electrodeposited Ni at: (a) 2, (b) 10, (c) 20, (d) 30, (e) 50 and (f) 100 mA cm^{-2} on copper substrate with a higher {111} peak intensity.

Therefore, spherical morphology is expected to obtain at lower current densities. But, at higher current densities, H_2 evolution becomes more intense and thus the pyramidal morphology gets a chance to be developed. The current density for this morphology transition is different on two copper substrates. This transition occurred at 50 mA cm^{-2} on copper substrate with a higher {111} peak intensity and at 30 mA cm^{-2} on the substrate with a higher {400} peak intensity. The different current density needed for morphology transition is most likely due to the difference in copper substrate texture. Due to the higher overpotential needed during Ni electrodeposition onto the copper substrate with a high {400} peak intensity, higher rate of H_2 evolution is expected on this substrate. Thus, the transition from spherical to pyramidal morphology happens at a lower current density (i.e. 30 mA cm^{-2}) on this substrate in respect to that (50 mA cm^{-2}) on copper substrate with a higher {111} peak intensity.

As seen in Figs. 3 and 4, the deposits formed onto the copper substrate with a higher {400}

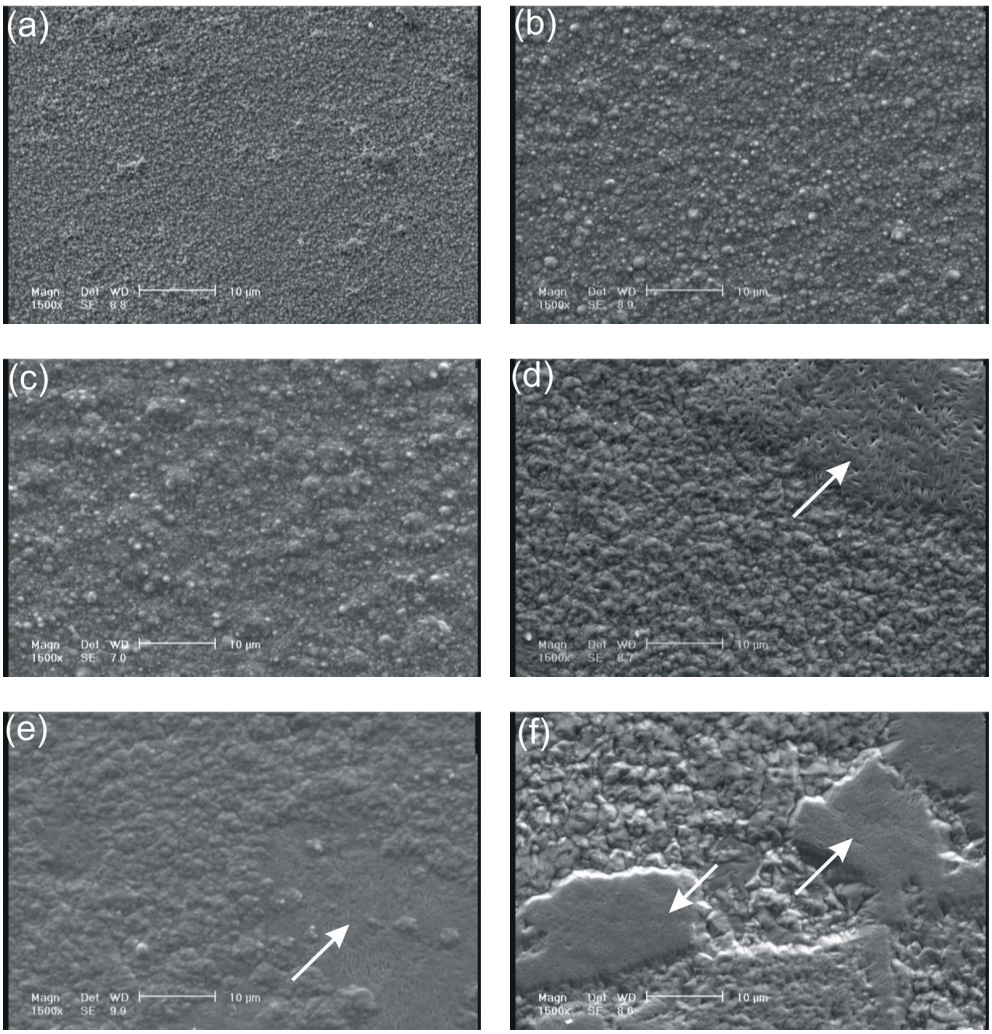

Fig. 4. Surface morphologies of electrodeposited Ni at: (a) 2, (b) 10, (c) 20, (d) 30, (e) 50 and (f) 100 mA cm^{-2} on copper substrate with a higher {400} peak intensity.

peak intensity show coarser morphology than on the copper substrate with a higher {111} peak intensity at the same current densities. This fact is due to the lower nucleation rate on the substrate with a high {400} peak intensity as discussed before. The results indicate that the morphology of deposit is strongly under the influence of substrate texture.

Figs. 5 and 6 show the X-ray peak intensity patterns of the as-deposited Ni coating at the mentioned current densities together with the annealed coating on the copper substrates with a higher {400} and {111} peak intensities, respectively. As seen from Figs. 5 and 6, in annealed coatings, the peaks are sharper indicating that the grain growth has occurred. In annealed deposit, the average grain size was around 2 μm.

Figs. 5 and 6 indicate that the electrodeposits consist of grains with a strong {220} peak intensity at lower current densities, but by increasing the current density, it is decreased and

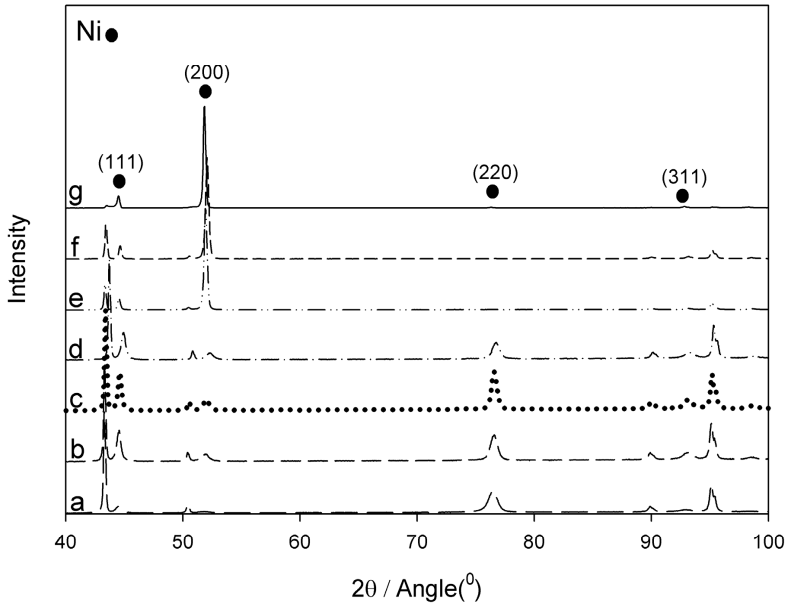

Fig. 5. XRD patterns of as-deposited nanocrystalline Ni at: (a) 2, (b) 10, (c) 20, (d) 30, (e) 50 and (f) 100 mA cm^{-2} on copper substrate with a higher {111} peak intensity and (g) annealed deposit.

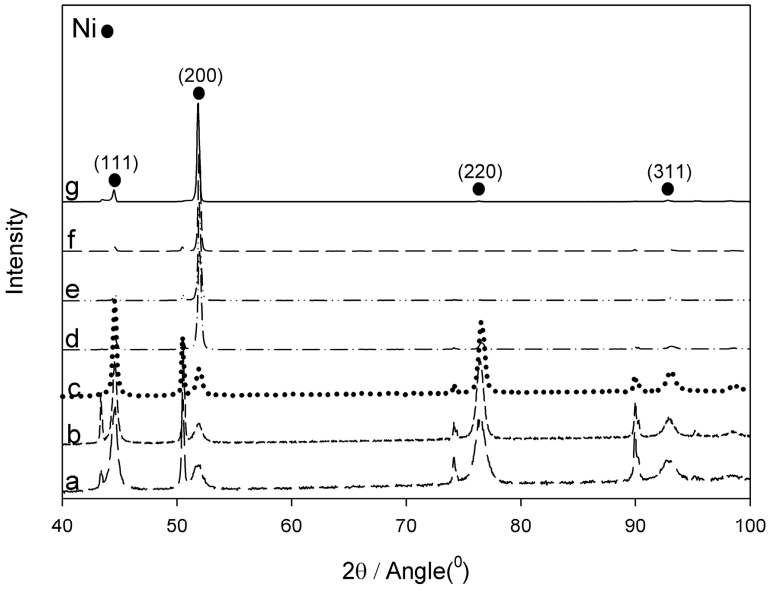

Fig. 6. XRD patterns of as-deposited nanocrystalline Ni at: (a) 2, (b) 10, (c) 20, (d) 30, (e) 50 and (f) 100 mA cm^{-2} on copper substrate with a higher {400} peak intensity and (g) annealed deposit.

it is eventually displaced by {200} peak intensity. This means that at low current density, the texture component of deposits is {220} but it changes to {200} at higher current densities. The texture coefficients of the coatings deposited onto both copper substrates at the mentioned current densities are calculated and shown in Figs. 7 and 8. The results are in a good agreement with the results of other studies [10, 11]. It is believed that at lower current densities, adsorption of H^+ is

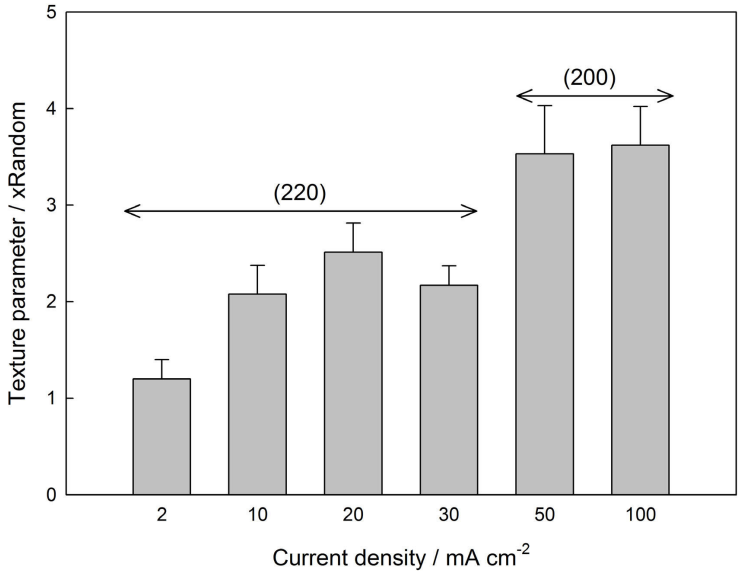

Fig. 7. Variation of texture coefficient (TC) with electrodeposition current density on copper substrate with a higher {111} peak intensity.

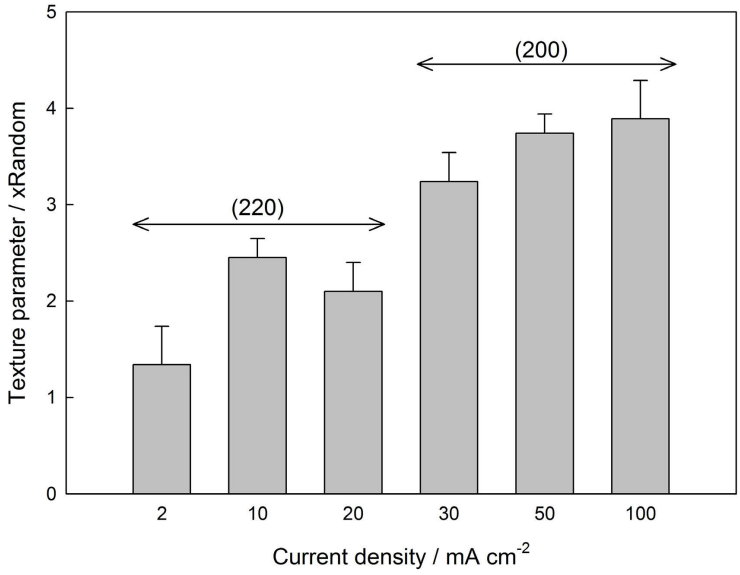

Fig. 8. Variation of texture coefficient (TC) with electrodeposition current density on copper substrate with a higher {400} peak intensity.

responsible for the formation of {220} texture component [10]. Increasing the current density reduces the adsorption of H+ and this leads to the formation of {200} texture component as mentioned by Chan et al. [10]. This texture transition which occurs by increasing the current density is in accordance to the morphology changes. This transition has happened again at 50 mA cm^{-2} on copper substrate with a higher {111} peak intensity and 30 mA cm^{-2} on substrate with a higher {400} peak intensity. These results show that H^+ should persist to remain adsorbed on

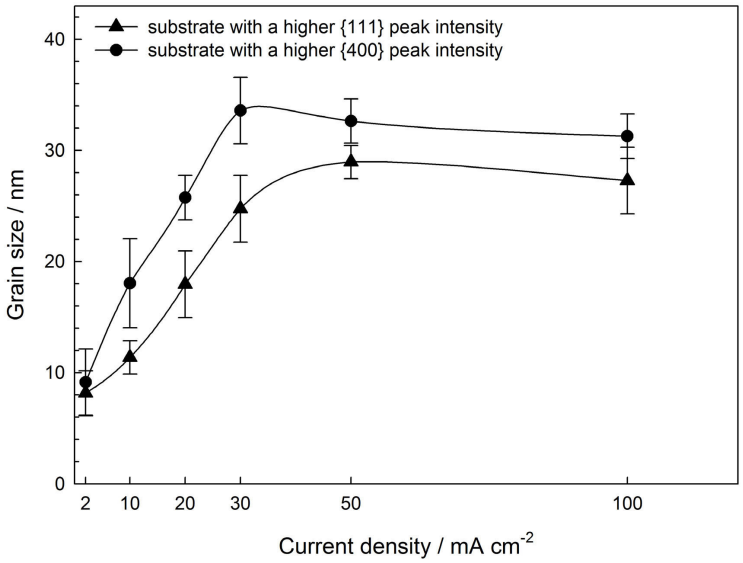

Fig. 9. Variation of grain size by electrodeposition current density on both copper substrates.

copper substrate with a higher {111} peak intensity. So, the change of texture should occur at a higher current density on the copper substrate with a higher {111} peak intensity.

Fig. 9 shows the variation of coating grain size with current density for two copper substrates. The grain size was calculated using the angular width of the Ni (200) peak at its FWHM in conjunction with the Scherrer equation [11]. The four-parameter Gaussian function was used for curve fitting analysis required for FWHM determination. Instrumental line broadening was also measured by a silicon standard specimen and corrected by the Gaussian–Cauchy equation. It has been shown that the grain size measured by the Gaussian–Cauchy equation is similar to what is obtained by TEM observations [4, 12]. According to Fig. 9, the as-deposited coatings resulted from Watt's bath have grain size in the range of 8 to 33 nm. The grain size increases with deposition current density on both copper substrates until it reaches to the current density where texture and morphology transforms, i.e. 30 mA cm^{-2} for copper substrate with a higher {400} peak intensity and 50 mA cm^{-2} for the substrate with a higher {111} peak intensity. After that the grain size remains almost constant without significant change with deposition current density. It has been mentioned [13, 14] that at low current density, a relatively small degree of Ni^{2+} depletion occurs at the cathode/electrolyte interface. Therefore, it could be assumed that a high Ni^{2+} ion concentration exists at the cathode surface which leads to a high degree of nucleation and result in a very fine-grained structure. However, the high nucleation rate can only explain why the crystallite size is small in the planes parallel to the substrate [13, 14]. During the layer deposition onto a substrate via atom-by-atom deposition process, a grain refinement can also occur if, for some reason, continuous crystal growth is stopped (inhibited) along the direction perpendicular to the growing surface [15]. In electrodeposition process, this inhibition can be caused by adsorption of some electrochemical species (or ions of the solution) on the growing crystal surface, which tends to inhibit growth normal to the substrate surface [13]. In the case of low deposition rate which occurs at low current density, it can be assumed that the probability of species adsorption on the growing crystal surface is fairly high [15] and therefore, the crystal growth can be frequently stopped. This retards the grain growth and leads to a very fine grain size in direction normal to the substrate surface. Hassani et al. [16] have investigated the grain growth in Ni-Co electrodeposition. They found that increasing the

current density encourages grain growth of Ni-Co electrodeposits and thus coarse grains can be achieved. Their results showed that the grain growth occurs by: (a) reducing the charge transfer resistance and thus increasing surface diffusion of adions and (b) preventing the adsorption of electrochemical species onto the active growth sites [16].

In Fig. 9, it is also clear that the grain size of deposit on the copper substrate with a higher {400} peak intensity is greater than on the copper substrate with a higher {111} peak intensity at the same current densities. As was mentioned before, the surface energy of {400} copper plane is higher than {111} plane and thus, nucleation rate on {400} plane is lower. Therefore, it can be assumed that the grain size of the coating on the copper substrate with a high {400} peak intensity is higher than on the substrate with a high {111} peak intensity.

3. 4. Corrosion Resistance of the Coatings

Tafel polarization plots for the coatings electrodeposited onto both copper substrates in 3.5 wt% NaCl solution are shown in Figs. 10 and 11. The corrosion parameters such as corrosion potential (E_{corr}), corrosion current density (i_{corr}), and Tafel slopes (β_a and β_c) were obtained from the polarization curves by using Tafel extrapolation method and are summarized in Tables 1 and 2. The exchange current density for cathodic (i_0^c) and anodic (i_0^a) reactions were obtained by extending the plateau portion of cathodic and anodic branches of Tafel plots to the reversible potentials of cathodic (i.e. water

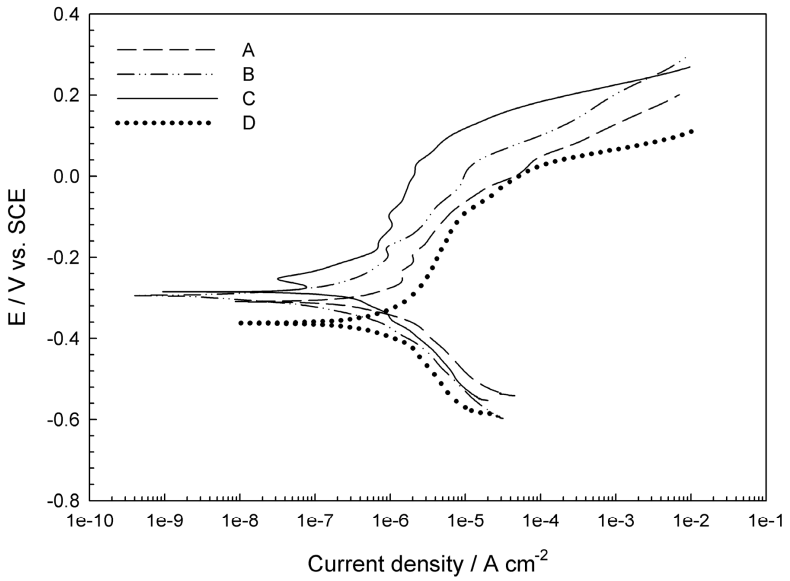

Fig. 10. Polarization curves of electrodeposited Ni with different current density in 3.5 wt% NaCl solution: (A) 10, (B) 30 and (C) 100 mA cm^{-2} on copper substrate with a higher {111} peak intensity and (D) annealed deposit.

Table 1. Corrosion parameters extracted from the plots in Fig. 10 using Tafel extrapolation.

Electrodeposition current density	Grain size (nm)	Microstrain (ε)	i_{corr} (μA cm^{-2})	E_{corr} (mV)	β_a (mV dec^{-1})	β_c (mV dec^{-1})	i_o^a (nA cm^{-2})	i_o^c (nA cm^{-2})
10 mA cm^{-2}	11.4±2	0.00513	0.8±0.2	-312±14	263±11	195±13	5±1	0.1±0.3
30 mA cm^{-2}	24.8±3	0.00477	0.5±0.1	-288±20	266±16	203±18	3.9±1	0.004±0.002
100 mA cm^{-2}	27.3±3	0.00440	0.3±0.1	-281±17	268±20	198±14	0.9±0.2	0.001±0.003
100 mA cm^{-2} +heat treatment	2000	-	1.3±0.5	-363±34	-	-	-	-

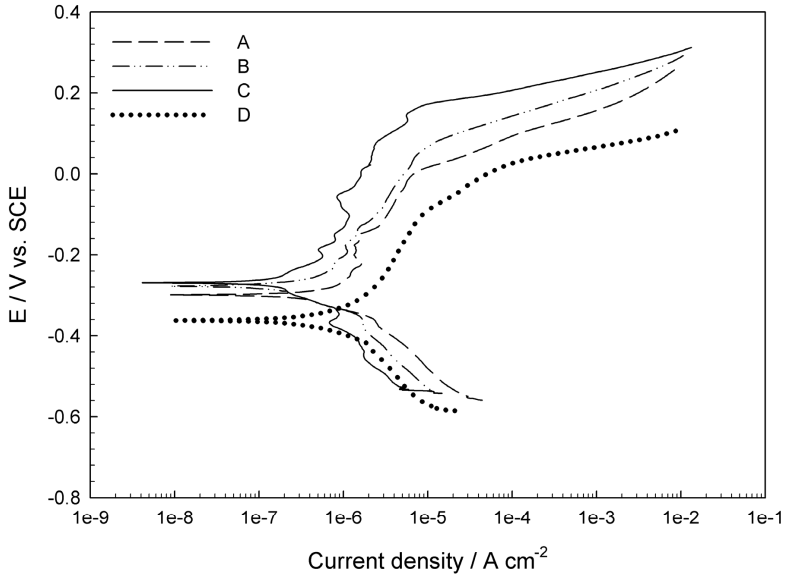

Fig. 11. Polarization curves of electrodeposited Ni with different current density in 3.5% NaCl solution: (A) 10, (B) 30 and (C) 100 mA cm^{-2} on substrate with a higher {400} peak intensity and (D) annealed deposit.

Table 2. Corrosion parameters extracted from the plots in Fig. 11 using Tafel extrapolation.

Electrodeposition current density	Grain size (nm)	Microstrain (ε)	i_{corr} (μA cm^{-2})	E_{corr} (mV)	β_a (mV dec^{-1})	β_c (mV dec^{-1})	i_o^a (nA cm^{-2})	i_o^c (nA cm^{-2})
10 mA cm^{-2}	18.1±4	0.00445	1±0.3	-300±12	305±16	200±17	7.5±0.5	0.11±0.1
30 mA cm^{-2}	33.6±3	0.00378	0.63±0.1	-275±18	307±19	207±20	6.3±0.8	0.002±0.002
100 mA cm^{-2}	31.3±3	0.00412	0.4±0.1	-264±15	308±20	200±14	0.6±0.4	0.001±0.002
100 mA cm^{-2} +heat treatment	2000	-	1.3±0.5	-363±34	-	-	-	-

reduction at the presence of oxygen (E^{H2O}) by assuming that it is the major cathodic reaction in NaCl solution) and anodic (i.e. reversible potential of nickel (E^{Ni})) reactions. These reversible potentials are about +500 and -760 mV, respectively.

The higher values of Ecorr obtained for nanocrystalline coatings in comparison to microcrystalline (2000 nm) coating show that by reducing the coating grain size to the nanometer scale, more noble values of potential are achieved. However, when the coating with 33.6 nm (Table 2) is compared with the coating with 11.4 nm grain size (Table 1), it is seen that E_{corr} is shifted slightly to the active potentials by this grain size reduction. This effect of grain size reduction on E_{corr} indicates that for the coatings with grains at nano-scale, other parameters rather than grain size are also important. In this case, surface morphology and texture seems to be the most important parameters.

According to Tables 1 and 2, corrosion rate of Ni nanocrystalline coatings are less than the microcrystalline coating. Although, this behaviour is consistent with the works of Wang et al. [4] and Mishra et al. [6], but it contradicts the classic corrosion theory which states that the nanostructures should accelerate corrosion by forming many more micro electrochemical cells between the huge amount of grain boundaries and the matrix. But, it should be noted that in this case, passive films are formed as it is evidenced from Tafel plots in Figs. 10 and 11. Youssef et al. [8] has suggested that the passive film formation

on the corroded surface of metal is a diffusion controlled process and it is expected that the diffusion of elements in nanocrystalline metals would be higher than that in microcrystallines and this facilitates the formation of passive films on nanocrystalline metals. It is reported that Ni nanocrystalline coatings have also a high density of nucleation sites for passive film formation which leads to the formation of a dense passive layer which results in very low corrosion rates. Therefore, it is expected that the corrosion resistance of Ni nanocrystalline in NaCl solution would be higher than that of microcrystalline. This may be also the reason for the fact that nanocrystalline Ni shows lower tendency for localized grain boundary corrosion [17].

Tables 1 and 2 show that β_a, β_c and ε are almost the same for the nanocrystalline coatings obtained at each current density and the only change is seen for the exchange current densities. Also it is noted in Tables 1 and 2 that both of the cathodic and anodic exchange current densities are decreased by increasing the deposition current density for both copper substrates. Therefore, the shift of Tafel plots to the left direction has happened by increasing the deposition current density without significant changes on the slopes. This results in a lower i_{corr} as seen from Tables 1 and 2. As discussed before, by increasing the deposition current density, the morphology and texture of the coating can be changed besides the increase in grain size. It seems that the decrease in i_{corr} by increasing the deposition current density from 10 to 30 $mAcm^{-2}$ is most probably due to the increase of grain size which its major effect is on decreasing the cathodic exchange current density (i_0^c). Further decrease in i_{corr} is resulted by increasing the current density of deposition to 100 $mAcm^{-2}$. As seen from Tables 1 and 2, the grain size is remained

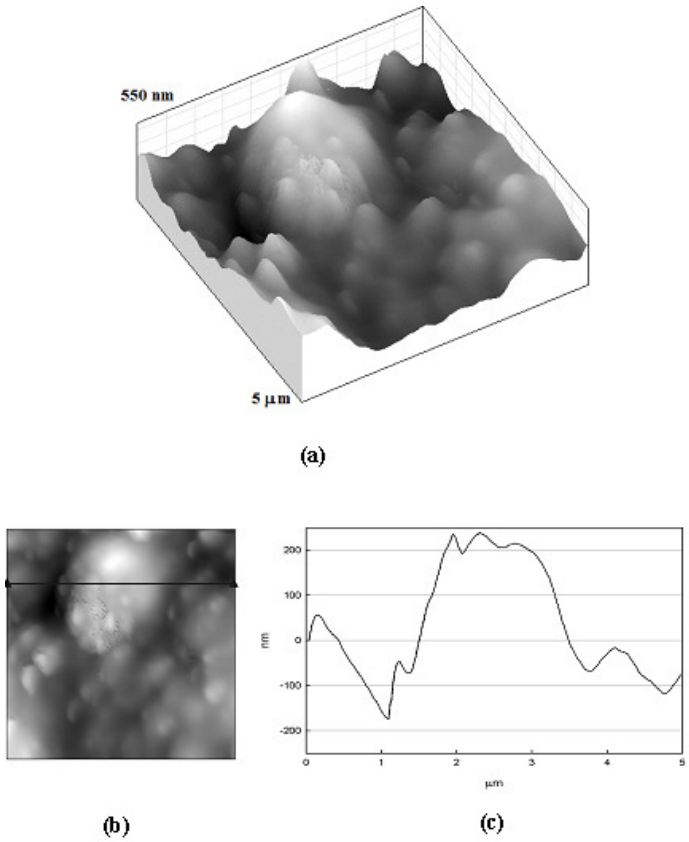

Fig. 12. AFM 3D image (a), top-view image (b) and section profilometry (c) of the coating deposited at 10 mA cm^{-2} onto the substrate with a higher {111} peak intensity.

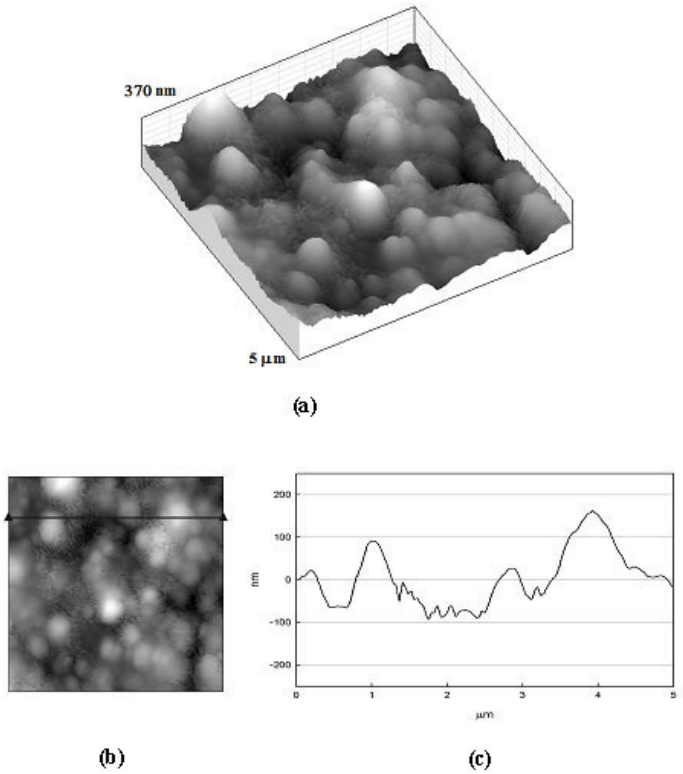

Fig. 13. AFM 3D image (a), top-view image (b) and section profilometry (c) on pyramidal region of the coating deposited at 100 mA cm^{-2} on the substrate with a higher {111} peak intensity.

almost constant by increasing the deposition current density from 30 to 100 $mAcm^{-2}$ on both copper substrates, but as discussed before, the morphology is changed. Therefore, the change of morphology from spherical to the mixed of pyramid and blocky is the major factor which has an influence on reducing the corrosion rate. This effect is due to the decrease of anodic exchange current density (i_0^a) which seems to be related to the presence of the blocky morphology in the surface structure of coating. It seems that a higher smoothness can be achieved by the presence of the blocky morphology which provides a lower value of exchange current density for anodic reactions. It can be assumed that the real exposure area (REA) of a coating to an aggressive solution is sensitive to the surface roughness and this area determines the value of anodic exchange current density. It seems that the value of REA is much lower for the blocky regions. Therefore, a lower value of i_0^a and consequently lower corrosion rate is obtained for the coating deposited at 100 mA cm^{-2} on both copper substrates.

In order to estimate the surface roughness of the coatings, AFM analysis was performed. The 3D image, top-view image and section profilometry of the coating deposited at 10 $mAcm^{-2}$ on copper substrate with a higher {111} peak intensity are shown in Fig. 12. Figs. 13 and 14 represents the results obtained for the coating produced at 100 mA cm^{-2} on the same substrate. The mentioned pyramidal and blocky regions are seen in Figs. 13 and 14, respectively. The roughness numbers including average roughness number (R_a), root mean square (RMS) and maximum height (R_z) obtained by profilometry are summarized in Table 3. The results show that by increasing the deposition current density, the Ra value decreases. Indeed, it can be seen from Table 3 that the roughness of the pyramidal region is more than the blocky region. This indicates that the presence of blocky morphology is reasonable for reducing the roughness.

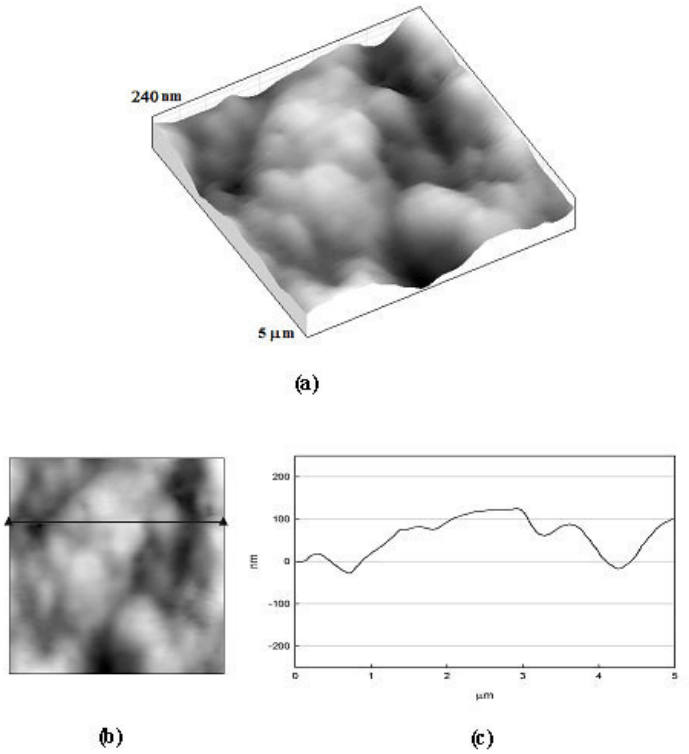

Fig. 14. AFM 3D image (a), top-view image (b) and section profilometry (c) on blocky region of the coating deposited at 100 mA cm^{-2} on the substrate with a higher {111} peak intensity.

Table 3. Tribological parameters extracted from AFM profilometries in Figs. 12-14.

Electrodeposition current density	10 mA cm^{-2}	100 mA cm^{-2}	
		Pyramidal regions	Blocky regions
R_a (nm)	79.2	42.9	33.9
RMS (nm)	97.1	54.9	41.0
R_z (nm)	476	338	193

4. CONCLUSIONS

1. Ni nanocrystalline electrodeposition onto the copper substrate with a high {400} peak intensity needs a higher overpotential with respect to the substrate with a high {111} peak intensity.
2. At 2 mA cm^{-2}, very fine grains with a spherical structure was obtained but at higher current densities, formation of pyramidal structure was encouraged and mixed morphology of pyramidal and blocky was pronounced.
3. The texture of copper substrate has a strong effect on grain size, texture and morphology of the obtained nanocrystalline Ni coatings.
4. E_{corr} was higher and i_{corr} was lower for the nanocrystalline coatings in respect to the microcrystalline.
5. The change of surface morphology from spherical to pyramidal corresponded to the texture variation from (220) to (200) which decreased the roughness and the anodic exchange current density and leads to a lower corrosion rate.
6. It should be noted that, although, numerous reports are concerning on the effect of deposition current density on corrosion resistance of Ni nanocrystalline electrodeposits,

but, the grain size has been attention as the only variable factor influencing the corrosion properties. In this research it was found that the effect of surface morphology can also be another factor.

REFERENCES

1. Peng, X., Zhang, Y., Zhao, J. and Wang, F., "Electrochemical corrosion performance in 3.5% NaCl of the electrodeposited nanocrystalline Ni films with and without dispersions of Cr nanoparticles." Electrochim. Acta, 2006, 51, 4922.
2. Rofagha, R., Langer, R., El-Sherik, A. M., Erb, U., Palumbo, G. and Aust, K. T., "The corrosion behaviour of nanocrystalline nickel." Scripta. Mater., 1991, 25, 2867.
3. Rofagha, R., Erb, U., Ostrander, D., Palumbo, G. and Aust, K. T., "The effects of grain size and phosphorus on the corrosion of nanocrystalline Ni-P alloys." Nanostruct. Mater., 1993, 2, 1.
4. Wang, L., Zhang, J., Gao, Y., Xue, Q., Hu, L., Xu, T., "Grain size effect in corrosion behavior of electrodeposited nanocrystalline Ni coatings in alkaline solution." Scripta. Mater., 2006, 55, 657.
5. Zhao, H., Liu, L., Zhu, J., Tang, Y., Hu, W., "Microstructure and corrosion behavior of electrodeposited nickel prepared from a sulphamate bath." Mater. Lett., 2007, 61, 1605.
6. Mishra, R., Balasubramaniam, R., "Effect of nanocrystalline grain size on the electrochemical and corrosion behavior of nickel." Corros. Sci., 2004, 46, 3019.
7. Ebrahimi, F., Ahmed, Z., "The effect of current density on properties of electrodeposited nanocrystalline nickel." J. App. Elechtrochem., 2003, 33, 733.
8. Porter, D. A. and Easterling, K. E., "Phase Transformation in Metals and Alloys," Chapman and Hall/CRC, Roca Raton, FL, 1992.
9. Karayannis, H. S., Patermarakis, G., "Effect of the Cl- and SO_4 2- ions on the selective orientation and structure of Ni electrodeposits." Electrochim. Acta, 1995, 40, 1079.
10. Chan, K. C., Qu, N. S. and Zhu. D., "Quantitative texture analysis in pulse reverse current electroforming of nickel." Surf. Coat. Technol., 1998, 99, 69.
11. Cullity, B. D., Stock, S. R. and Stock S., "Elements of x-ray diffraction," Addision-Wesley, London, 2001.
12. Wu, B. Y. C., "Synthesis and characterization of nanocrystalline alloys in the binary Ni–Co system," M. Sc. thesis, University of Toronto, 2002.
13. Bakonyi, I., Toth-Kadar, E., Pogany, L., Cziraki, A., Gerocs, I., Varga-Josepovits, K., Arnold, B., Wetzig, K., "Preparation and characterization of d.c.-plated nanocrystalline nickel electrodeposits." Surf. Coat. Technol., 78 (1996) 124.
14. Chin, D-T., "Mass transfer and current-potential relation in pulse electrolysis." J. Electrochem. Soc., 1983, 130, 1657.
15. Winand, R., "Electrodeposition of metals and alloys-new results and perspectives." Electrochim. Acta, 1994, 39, 1091.
16. Hassani, Sh., Raeissi K. and Golozar, M. A., "Effects of saccharin on the electrodeposition of Ni-Co nanocrystalline coatings." J. Appl. Electrochem., 2008, 38, 689.
17. Wang, L., Gao, Y., Xue, Q., Liu, H. and Xu, T., "Graded composition and structure in nanocrystalline Ni-Co alloys for decreasing internal stress and improving tribological properties." J. Phys D: Appl. Phys., 2005, 38, 1318.